Conditioned medium of PC-3 prostate cancer cells affects microRNA and mRNA profiles in mechanically strained osteoblasts

ZHEN CAO[1-3], ZHIXIONG YAN[1,2], JIAHUI WANG[1,2], HUAN YANG[1,2], BIAO HAN[1,2], JINTAO GAO[1,2] and YONG GUO[1,2]

[1]Department of Biomedical Engineering, College of Biotechnology, Guilin Medical University, Guilin; [2]Key Laboratory of Biochemistry and Molecular Biology, Guilin Medical University, Education Department of Guangxi Zhuang Autonomous Region, Guilin, Guangxi 541199; [3]Department of Histology & Embryology, College of Basic Medical Sciences, Dalian Medical University, Dalian, Liaoning 116044, P.R. China

Received August 22, 2022; Accepted January 16, 2023

DOI: 10.3892/etm.2023.11837

Abstract. Bone is the main site of metastasis from prostate cancer; therefore, it is important to investigate the microRNAs (miRNAs) and mRNA associated with bone metastases from prostate cancer. Since an appropriate mechanical environment is important in the growth of bone, in the present study, the miRNA, mRNA, and long non-coding RNA (lncRNA) profiles of mechanically strained osteoblasts treated with conditioned medium (CM) from PC-3 prostate cancer cells were studied. MC3T3-E1 osteoblastic cells were treated with the CM of PC-3 prostate cancer cells and were simultaneously stimulated with a mechanical tensile strain of 2,500 $\mu\varepsilon$ at 0.5 Hz; the osteoblastic differentiation of the MC3T3-E1 cells was then assessed. In addition, the differential expression levels of mRNA, miRNA and lncRNA in MC3T3-E1 cells treated with the CM of PC-3 cells were screened, and some of the miRNAs and mRNAs were verified by reverse transcription-quantitative PCR (RT-qPCR). The signal molecules and signaling pathways associated with osteogenic differentiation were predicted by bioinformatics analysis. The CM of PC-3 prostate cancer cells suppressed osteoblastic differentiation of MC3T3-E1 cells. A total of seven upregulated miRNAs and 12 downregulated miRNAs were selected by sequencing and further verified using RT-qPCR, and related differentially expressed genes (11 upregulated and 12 downregulated genes) were also selected by sequencing and further verified using RT-qPCR; subsequently, according to the enrichment of differentially expressed genes in signaling pathways, nine signaling pathways involved in osteogenic differentiation were screened out. Furthermore, a functional mRNA-miRNA-lncRNA regulatory network was constructed. The differentially expressed miRNAs, mRNAs and lncRNAs may provide a novel signature in bone metastases of prostate cancer. Notably, some of the signaling pathways and related genes may be associated with pathological osteogenic differentiation caused by bone metastasis of prostate cancer.

Correspondence to: Dr Yong Guo, Department of Biomedical Engineering, College of Biotechnology, Guilin Medical University, 1 Zhiyuan Road, Lingui, Guilin, Guangxi 541199, P.R. China
E-mail: guoyong74@163.com

Key words: prostate cancer, mechanically strained, osteoblasts, microRNA, mRNA

Introduction

Bone is associated with electrolyte balance, energy metabolism and mechanical competence; it performs these functions through a continuous homeostatic balance between modeling and remodeling processes that is carried out mainly by osteoblasts (OBs) and osteoclasts (OCs), which act via bone formation and resorption, respectively (1). Prostate cancer is a common malignant tumor that can be fatal for male patients with advanced tumors, and it is also one of the malignant tumors most associated with bone metastasis (2). The common metastasis of prostate cancer cells to bone can disrupt bone remodeling, and results in lesions that cause significant pain and patient morbidity (3,4). Therefore, it is of great significance to study the mechanism underlying pathological bone formation and osteogenic differentiation caused by prostate cancer bone metastases. However, effective therapies for bone metastatic disease are underdeveloped, and the majority of therapies are palliative with only a modest survival benefit (3,5). The exact mechanisms underlying the metastasis of prostate cancer to the bone are unclear. However, evidence has suggested that the bone marrow microenvironment, particularly its related microRNAs (miRNAs/miRs) and pathways, is a significant factor of prostate cancer bone metastasis (6,7).

Bone metastasis of prostate cancer leads to abnormal osteoblastic differentiation, and causes fatal osteolytic and osteoblastic abrasions, which results in a poor quality of life in individuals with prostate cancer (8,9). The development of either osteolytic or osteoblastic lesions caused by prostate cancer bone metastasis results from functional interactions

between tumor cells and osteoclasts or osteoblasts, respectively (10). Therefore, it is important to investigate the effect of prostate cancer cells on osteoblasts or osteoclasts *in vitro* or *in vivo*.

The growth of bone requires an appropriate mechanical environment, osteoblasts, important functional cells in bone, are usually stimulated by a mechanically loaded, and there is a dynamic balance between bone resorption and bone formation (11). Physiological bone formation and osteogenic differentiation is induced by osteoblasts under physiological mechanical loads. The physiological strain of human weight-bearing bone is generally <2,000 $\mu\varepsilon$ (12). In Frost's bone function adaptability model, 50-2,500 $\mu\varepsilon$ is considered strain in the physiological range (13,14). Previous studies of osteoblasts cultured *in vitro* revealed that mechanical tensile strain of 2,500 $\mu\varepsilon$ at 0.5 Hz could promote osteogenic differentiation and improve osteogenic function (15-17), and that mechanical tensile strain of 2,500 $\mu\varepsilon$ at 0.5 Hz could be regarded as normal physiological load (17). Under normal physiological load, the abnormal osteogenic differentiation caused by bone metastasis of prostate cancer is regarded as pathological osteogenic differentiation. Therefore, in the present study, *in vitro* osteoblasts were stimulated with physiological mechanical strain and were simultaneously treated with the condition medium (CM) of prostate cancer cells; this is considered a good cell model of bone metastasis from prostate cancer.

In the present study, the MC3T3-E1 osteoblastic cells were treated with the CM of prostate cancer cells and physiological mechanical tensile strain (2,500 $\mu\varepsilon$ at 0.5 Hz) was simultaneously applied to the cells using a four-point bending device. Subsequently, the osteogenic differentiation of cells under the conditions of pathology (CM and physiological mechanical strain) and physiology (fresh medium and physiological mechanical strain) were detected. The differentially expressed mRNAs and miRNAs in the pathology group were detected and verified by high-throughput RNA sequencing and reverse transcription-quantitative PCR (RT-qPCR). Finally, bioinformatics technology was used to screen and predict the signal molecules and signaling pathways related to bone metastasis.

Materials and methods

Preparation of CM. PC-3 prostate cancer cells (American Type Culture Collection) were cultured in Dulbecco's modified Eagle's medium (DMEM; Gibco; Thermo Fisher Scientific, Inc.) containing 10% fetal bovine serum (FBS; Gibco; Thermo Fisher Scientific, Inc.) in an incubator containing 5% CO_2 at 37˚C. PC-3 cells ($1x10^6$) were grown in a 25-cm^2 culture flask in cell culture medium until 60-70% confluent. After two washes with phosphate-buffered saline (PBS), cells were incubated in DMEM containing 1% FBS for 48 h, and the crude CM (CCM) was then collected, filtered through a 0.2-μm sterilizing filter and stored at -80˚C. The PC-3 CM contained 20% PC-3 CCM, and 80% DMEM containing 10% FBS (FBS; Gibco; Thermo Fisher Scientific, Inc.) culture medium.

PC-3 CM treatment and mechanical stimulus. The MC3T3-E1 mouse pre-osteoblastic cell line (provided by the Institute of Basic Medicine of Peking Union Medical College, Beijing, China), at the third passage, was seeded into mechanical loading dishes, which were reformed from cell culture dishes (Nunc; Thermo Fisher Scientific, Inc.) in DMEM supplemented with 10% FBS and 1% penicillin-streptomycin (Gibco; Thermo Fisher Scientific, Inc.), mechanical loading dishes were reformed from cell culture dishes (Nunc; Thermo Fisher Scientific, Inc.) according to the previously described method (17).

At 100% confluence, the medium was replaced with the PC-3 CM in the pathological group and with DMEM in the physiological group. All of the MC3T3-E1 cells were subjected to a mechanical tensile strain of 2,500 $\mu\varepsilon$ at 0.5 Hz, 1 h/day for 3 days. The mechanical strain was generated using a specially designed four-point bending device (provided by The Institute of Medical Equipment, Academy of Military Medical Sciences, Tianjin, China), as previously described (17).

Alkaline phosphatase (ALP) activity assay. After treatment with CM and mechanical stimulation, the MC3T3-E1 cells were lysed by brief sonication at 20 kHz for 1 min on ice in radioimmunoprecipitation (RIPA) lysis buffer (CW Biosciences). The protein concentration of the cell lysates was measured using the Bicinchoninic Acid (BCA) Protein Assay kit (CW Biosciences). ALP activity in the lysates was subsequently measured with an alkaline phosphatase assay kit (cat. no. A059-2-1; Nanjing Jiancheng Bioengineering Institute) using the p-nitrophenyl phosphate method, according to the manufacturer's instructions.

ALP and alizarin red-S staining. Following treatment, the cells were washed with PBS and fixed with 4% paraformaldehyde for 20 min at 37˚C. The fixed cells were incubated with the ALP staining kit (cat. no. D001-2-1; Nanjing Jiancheng Bioengineering Institute) and Alizarin red-S staining kit (cat. no. C0148; Beyotime Institute of Biotechnology) to reveal the calcium deposition of cells, according to the manufacturer's instructions. Cells were then observed under an optical microscope.

Western blotting. Following treatment, the protein extracts of the cells were harvested in RIPA lysis buffer (Beijing Solarbio Science & Technology Co., Ltd.) and protein concentration in the cell lysates was quantified using the BCA Protein Assay kit. Proteins (15 μg) were then separated by SDS-PAGE on 10% gels and transferred to nitrocellulose membranes, which were blocked with 2.5% BSA (Beijing Solarbio Science & Technology Co., Ltd.) in Tris-buffered saline with 0.1% Tween-20 (Beijing Solarbio Science & Technology Co., Ltd.) at room temperature for 2 h. Membranes were then incubated with the following primary antibodies at 4˚C for 15 h: Anti-RUNX-2 (1:200; cat. no. sc-390351) and anti-β-actin (1:1,000; cat. no. sc-8432) (both from Santa Cruz Biotechnology, Inc.). The membranes were then incubated with horseradish peroxidase-conjugated secondary antibodies (1:2,000; cat. no. sc-2005; Santa Cruz Biotechnology, Inc.) at 37˚C for 1 h. Immunoreactive bands were detected using an enhanced chemiluminescence detection reagent (Pierce; Thermo Fisher Scientific, Inc.). β-actin in the cell lysates was used as a loading control and data were normalized against the corresponding optical density of β-actin. ImageJ 1.48 software (National Institutes of Health) was used for semi-quantification of bands.

Table I. Primer sequence for all mRNAs.

mRNA	Primer sequences, 5'-3'
Col I	F: GGTATGCTTGATCTGTATCT
	R: TCTTCTGAGTTTGGTGATACG
OCN	F: AGTCTGACAAAGCCTTCA
	R: AAGCAGGGTTAAGCTCACA
Nr4a1	F: TGGTGAAGGAAGTTGTGCGT
	R: ATCAAGGTCTCTGGGCGTTG
Porcn	F: CTACGAGCCTACGAGAGTGCT
	R: CTGTGGCCTCAGACAGAAAGC
Angpt1	F: ATCCCGACTTGAAATACAACTGC
	R: CTGGATGATGAATGTCTGACGAG
Lef1	F: GCCACCGATGAGATGATCCC
	R: TTGATGTCGGCTAAGTCGCC
Fos	F: CGGGTTTCAACGCCGACTA
	R: TGGCACTAGAGACGGACAGAT
Cdca8	F: AAAAGCGAAAGGTAATCGAGGT
	R: TGCAGATCGAAGATTCTTATGGC
Bcl3	F: CCGGAGGCCCTTTACTACCA
	R: GGAGTAGGGGTGAGTAGGCAG
Fosb	F: CCTCCGCCGAGTCTCAGTA
	R: CCTGGCATGTCATAAGGGTCA
Bdkrb1	F: CCCCTCCCAACATCACCTC
	R: GGACAGGACTAAAAGGTTCCCC
Osmr	F: GCATCCCGAAGCGAAGTCTT
	R: GGGCTGGGACAGTCCATTCTA
Podn	F: GACTGTCCCCGAGATTGTGC
	R: CAGGTCGCCTGGAAACTCA
Prc1	F: AACTCACCTCCGGGAAATATGG
	R: GGATATGCTTTTGAGCAGCCT
Pfkfb3	F: CAACTCCCCAACCGTGATTGT
	R: TGAGGTAGCGAGTCAGCTTCT
Nos2	F: GTTCTCAGCCCAACAATACAAGA
	R: GTGGACGGGTCGATGTCAC
Tnnc1	F: GCGGTAGAACAGTTGACAGAG
	R: GACAAGAAACTCATCGAAGTCCA
Slc6a2	F: TTCTGGCGCGAATGAATCC
	R: AGTAGATCGGCGGTTTTGCAG
Nfatc2	F: TCATCCAACAACAGACTGCCC
	R: GGGAGGGAGGTCCTGAAAACT
Tnc	F: TTTGCCCTCACTCCCGAAG
	R: AGGGTCATGTTTAGCCCACTC
Car9	F: GGTTAGAGGATCTATCGACTCCC
	R: GGTGCCTCCATAGCTCCAA
Timp1	F: CGAGACCACCTTATACCAGCG
	R: ATGACTGGGGTGTAGGCGTA
Kif23	F: ATGAAGTCAGCGAAGGCTAAGA
	R: GCGAACCCTACAGTACACCC
Angpt4	F: CAGCCAGCTATGCTACTAGATGG
	R: CAGGCAAGTCCCTCTGGAG
Cdc25c	F: GTTTCAGCACCCAGTTTTAGGT
	R: AGAATGCTTAGGTTTGCCGAG
Mmp3	F: GGCCTGGAACAGTCTTGGC
	R: TGTCCATCGTTCATCATCGTCA
Prc	F: GAGTCAGTCACAACAGATGC
	R: TGCACAAGATACACCTTCATCC
β-actin	F: CACCATTGGCAATGAGCGGTTC
	R: AGGTCTTTGCGGATGTCCACGT

F, forward; R, reverse.

Preparation of total RNA and cDNA for small RNA sequencing. Total RNA was isolated from cells using TRIzol® reagent (Invitrogen; Thermo Fisher Scientific, Inc.) according to the manufacturer's protocol. RNA purity was assessed using the ND-1000 Nanodrop (NanoDrop; Thermo Fisher Scientific, Inc.). Each RNA sample had an A260:A280 ratio >1.8 and an A260:A230 ratio >2.0. RNA integrity was evaluated using the Agilent 2200 TapeStation (Agilent Technologies, Inc.) and each sample had the RNA integrity number >7.0. Briefly, RNA molecules were ligated with a 3' RNA adapter, followed by 5' adapter ligation, using a Truseq™ Small RNA sample prep Kit (cat. no. RS-200-0012; Illumina, Inc.). Subsequently, the adapter-ligated RNAs were reversed transcribed to cDNA and PCR amplified. cDNA was synthesized using an AmpliSeq cDNA Synthesis for Illumina kit (cat. no. 20022654; Illumina, Inc.), the thermocycling conditions used for reverse transcription were 12˚C for 15 min and 95˚C for 3 min. PCR amplification was performed using the Illumina® DNA PCR-Free Sequencing and Indexing Primer kit (cat. no. 20041797; Illumina, Inc.), the thermocycling conditions for PCR amplification were 94˚C for 180 sec, followed by 20 cycles of 98˚C for 20 sec, annealing at 56˚C for 15 sec and extension at 72˚C for 15 sec. Subsequently, the size of PCR products was selected by PAGE gel according to the instructions of the NEBNext® Multiplex Small RNA Library Prep Set for Illumina® (cat. no. E7330S; New England Biolabs, Inc.). The purified library products were evaluated using the Agilent 2200 TapeStation and the Qubit® 2.0 Fluorometer (Invitrogen; Thermo Fisher Scientific, Inc.), then diluted to 2 pM for sequencing. The type of sequencing performed was single-end from 3' ends and 50 bp was sequenced each time using HiSeq X Reagent Kits (cat. no. FC-501-2501; Illumina, Inc.).

Differential expression analysis was conducted using miRDeep2 (v2.0.0) software (18). A miRNA with 'P-adjust' <0.05 and |log2FC|≥1.0 compared with the physiological group was considered to be differentially expressed.

Preparation of total RNA and cDNA for transcriptome sequencing. Briefly, the total RNA quality was assessed as in the previous subsection, rRNAs were removed from total RNA using Epicentre Ribo-Zero rRNA Removal Kit (Illumina, Inc.) and fragmented to ~200 bp. Subsequently, the purified RNAs were subjected to first strand and second strand cDNA synthesis according to the aforementioned method, followed by adaptor ligation and enrichment with a low-cycle according to instructions of the NEBNext®

Table II. Primer sequences of all miRNAs.

miRNA	miRBase accession no.	Primer sequence, 5'-3'
mmu-miR-190b-5p	MIMAT0004852	TGATATGTTTGATATTGGGTT
mmu-miR-296-5p	MIMAT0000374	AGGGCCCCCCCTCAATCCTGT
mmu-miR-33-5p	MIMAT0000667	GTGCATTGTAGTTGCATTGCA
mmu-miR-1224-3p	MIMAT0017231	CCCCACCTCTTCTCTCCTCAG
mmu-miR-3963	MIMAT0019341	TGTATCCCACTTCTGACAC
mmu-miR-3473d	MIMAT0020632	CCACTGAGCCACTTTCCAGCCCTT
mmu-miR-219c-5p	MIMAT0029892	GGACGTCCAGACGCAACTCTCG
mmu-miR-505-3p	MIMAT0003513	CGTCAACACTTGCTGGTTTTCT
mmu-miR-467h	MIMAT0005855	ATAAGTGTGTGCATGTATATGT
mmu-miR-96-5p	MIMAT0000541	TTTGGCACTAGCACATTTTTGCT
mmu-miR-466m-3p	MIMAT0014883	TACATACACACATACACACGCA
mmu-miR-466j	MIMAT0005848	TGTGTGCATGTGCATGTGTGTAA
mmu-miR-542-5p	MIMAT0003171	CTCGGGGATCATCATGTCACGA
mmu-miR-6412	MIMAT0025165	TCGAAACCATCCTCAGCTACTA
mmu-miR-181a-2-3p	MIMAT0005443	ACCGACCGTTGACTGTACCTTG
mmu-miR-133a-3p	MIMAT0000145	TTTGGTCCCCTTCAACCAGCTG
mmu-miR-470-5p	MIMAT0002111	TTCTTGGACTGGCACTGGTGAGT
mmu-miR-497b	MIMAT0031404	CACCACAGTGTGGTTTGGACGTGG
mmu-miR-7083-5p	MIMAT0028072	TCGGGGCTGGACAAGCAGAGA
mmu-miR-9-3p	MIMAT0000143	ATAAAGCTAGATAACCGAAAGT
mmu-miR-3061-3p	MIMAT0014829	CTACCTTTGATAGTCCACTGCC
mmu-miR-217-5p	MIMAT0000679	TACTGCATCAGGAACTGACTGGA
mmu-miR-499-5p	MIMAT0003482	TTAAGACTTGCAGTGATGTTT
Universal reverse primer		GTGCAGGGTCCGAGGT
U6		F: CTCGCTTCGGCAGCACA
		R: AACGCTTCACGAATTTGCGT

miR/miRNA, microRNA; F, forward; R, reverse.

Ultra™ Directional RNA Library Prep Kit for Illumina (cat. no. E7420L; New England Biolabs, Inc.). The purified library products were evaluated using the Agilent 2200 TapeStation and Qubit 2.0 Fluorometer, and the final library was diluted to 10 pM for sequencing. The type of sequencing was paired-end from 3' ends and 150 bp was sequenced each time using HiSeq X Reagent Kits.

The differential expression analysis was conducted using DEGseq 1.38.0 software (19). Genes with 'P-adjust'<0.05 and |log2FC|≥1.0 compared with the physiological group were considered differentially expressed genes.

RT-qPCR for mRNA and miRNA. RT-qPCR was performed to further validate selected differentially expressed mRNAs and miRNAs identified from small RNA sequencing and transcriptome sequencing.

Total RNA was isolated from cells using TRIzol reagent, according to the manufacturer's protocol. After total RNA was extracted from the cells, cDNA was synthesized using a Quant Script RT kit (Tiangen Biotech Co., Ltd.); the thermocycling conditions for RT were 12˚C for 15 min and 95˚C for 3 min. qPCR was performed to detect the mRNA expression levels using SYBR Green I PCR mix (CW Biosciences) on a Real-Time PCR system (7900; Applied Biosystems; Thermo Fisher Scientific, Inc.), according to the manufacturer's instructions. The amplification reaction included a

Table III. Enrichment analyses of KEGG pathway identified certain signaling pathways related to osteoblastic differentiation.

Target pathway	Target genes
'Wnt signaling pathway'	Nfatc2, Lef1, Porcn
'MAPK signaling pathway'	Nr4a1, Dusp6, Cdc25b, Fos
'Calcium signaling pathway'	Bdkrb1, Sphk1, Nos2, Tnnc1
'Osteoclast differentiation'	Nfatc2, Fosb, Fos
'Pathways in cancer'	Bdkrb1, Il6, Nos2, Lef1, Fos
'TNF signaling pathway'	Mmp3, Il6, Fos, Bcl3
'HIF-1 signaling pathway'	Angpt1, Angpt4, Timp1, Nos2, Pfkfb3, Il6
'MicroRNAs in cancer'	Tnc, Cdc25c, Kif23, Cdc25b
'Rheumatoid arthritis'	Mmp3, Cxcl5, Angpt1, Il6, Fos

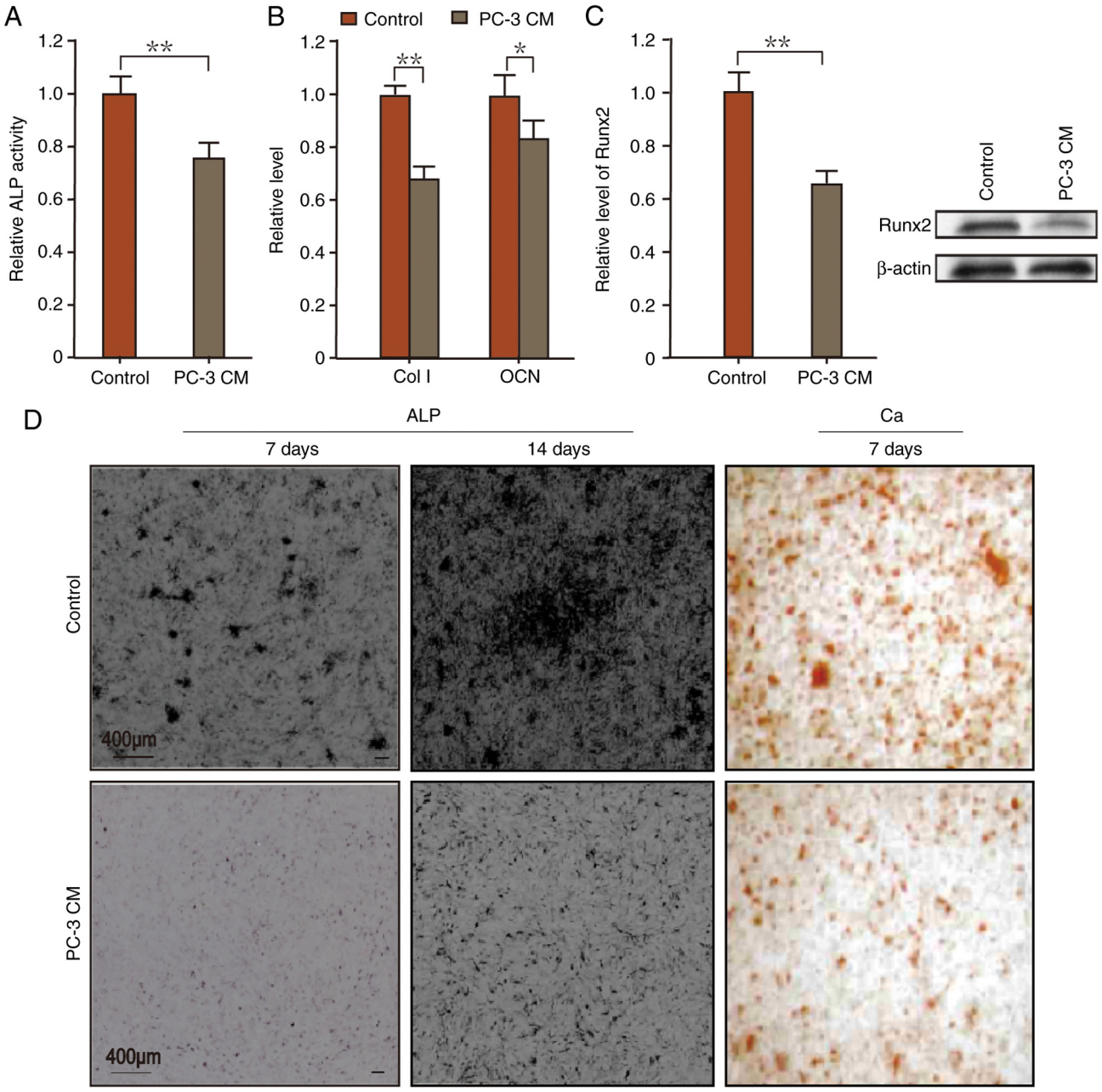

Figure 1. Osteoblastic differentiation of MC3T3-E1 cells treated with PC-3 CM and stimulated with mechanical strain. All of the MC3T3-E1 cells were stimulated with a mechanical tensile strain of 2,500 $\mu\varepsilon$ at 0.5 Hz. PC-3 CM decreased the (A) ALP activity, (B) mRNA expression levels of Col and OCN, (C) Runx2 protein expression levels and (D) the activity of ALP and Ca deposition of the MC3T3-E1 cells. *P<0.05 and **P<0.01 vs. control group (only stimulated with mechanical strain). ALP, alkaline phosphatase; Ca, calcium; CM, conditioned medium; Col I, collagen I; OCN, ostocalcin.

denaturation step at 94˚C for 180 sec, followed by 40 cycles of 94˚C for 15 sec, annealing and extension at 60˚C for 30 sec. Each sample was analyzed in triplicate. The expression levels of mRNA were normalized to the internal control β-actin using the $2^{-\Delta\Delta Cq}$ method (20). The mRNA primer sequences are shown in Table I.

The miRNA expression levels were assessed using RT-qPCR by Guangzhou Ribobio Co., Ltd. The miRNA Uni-Reverse Primers and miRNA Primers (specific primers) for RT-qPCR of miRNA were provided by Guangzhou Ribobio Co., Ltd. Poly(A) tailing. Total RNA was isolated from cells using TRIzol reagent, according to the manufacturer's protocol. After total RNA was extracted from the cells cDNA was synthesized by reverse transcription according to the aforementioned method and qPCR was successively performed using the miDETECT A Track miRNA qRT-PCR Starter Kit (Guangzhou Ribobio Co., Ltd.). The reactions were incubated in a 96-well optical plate at 95˚C for 20 sec, followed by 40 cycles of 10 sec at 95˚C, 20 sec at 60˚C and 10 sec at 70˚C. The miRNA expression levels were normalized to U6 snRNA. The miRNA primer sequences are shown in Table II.

Competing endogenous RNA (CeRNA) network. According to the results of the differential expression analysis, the regulatory relationships between long non-coding RNA (lncRNA) and miRNA were predicted using miRanda (http://cbio.

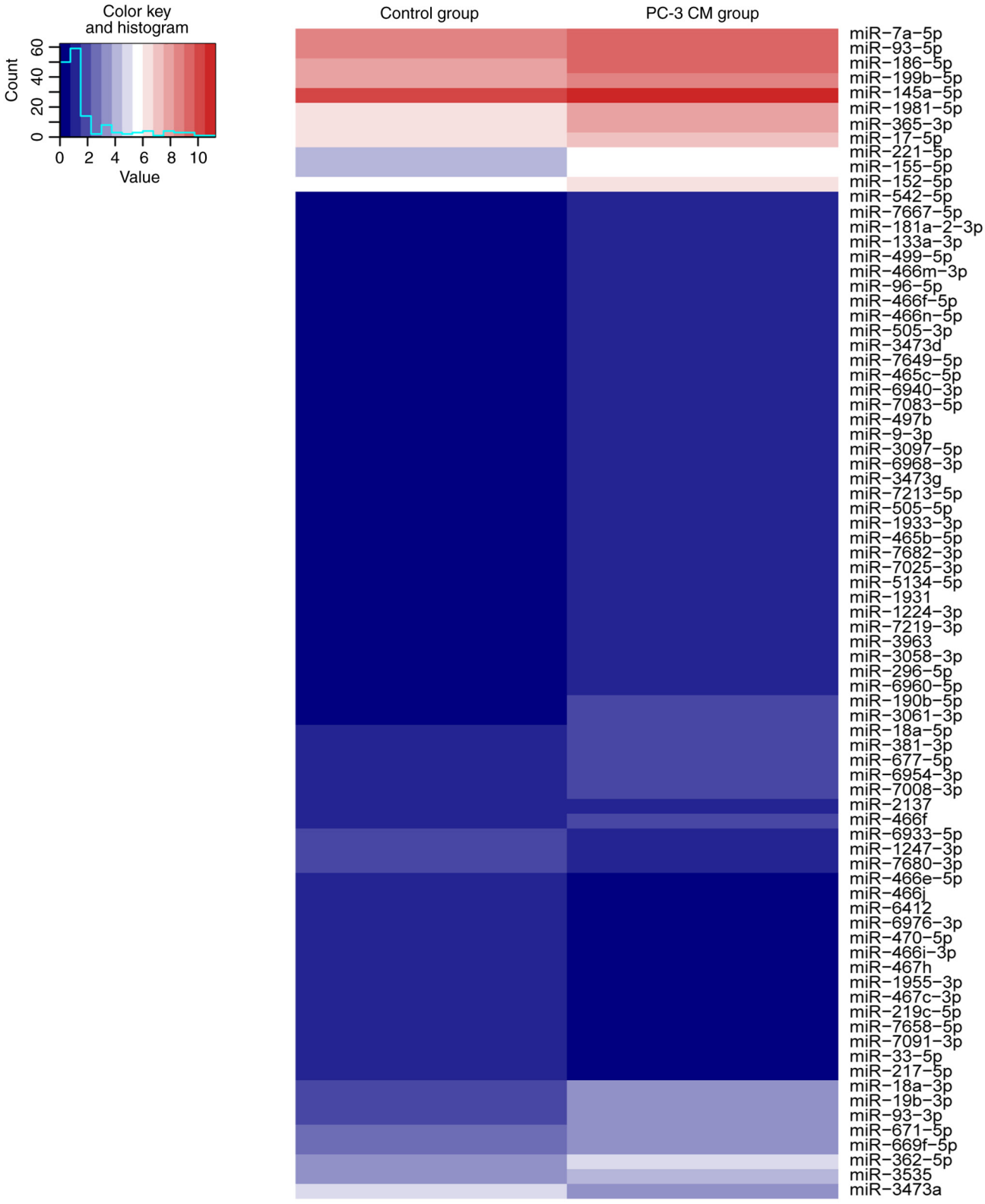

Figure 2. Heat map of differentially expressed miRNAs from MC3T3-E1 cells subjected to mechanical tensile strain and treated with PC-3 CM, as determined by RNA sequencing. Control group, stimulated with mechanical strain; PC-3 CM group, stimulated with mechanical strain and treated with PC-3 CM. The colors represent relative levels of miRNAs. CM, conditioned medium; miRNA/miR, microRNA.

mskcc.org/miRNA2003/miranda.html), pictar (https://pictar.mdc-berlin.de/) and RNAhybrid (https://bibiserv.cebitec.uni-bielefeld.de/rnahybrid/). The prediction results of these three types of software were used as the candidate lncRNA, which acts as a sponge of miRNAs, the expression of lncRNAs reduces the expression of corresponding miRNAs. Therefore, the present study selected the lncRNA-miRNA pairs where the expression patterns between lncRNAs and miRNAs were different. In addition, significant differentially expressed miRNAs and mRNAs were extracted to construct the

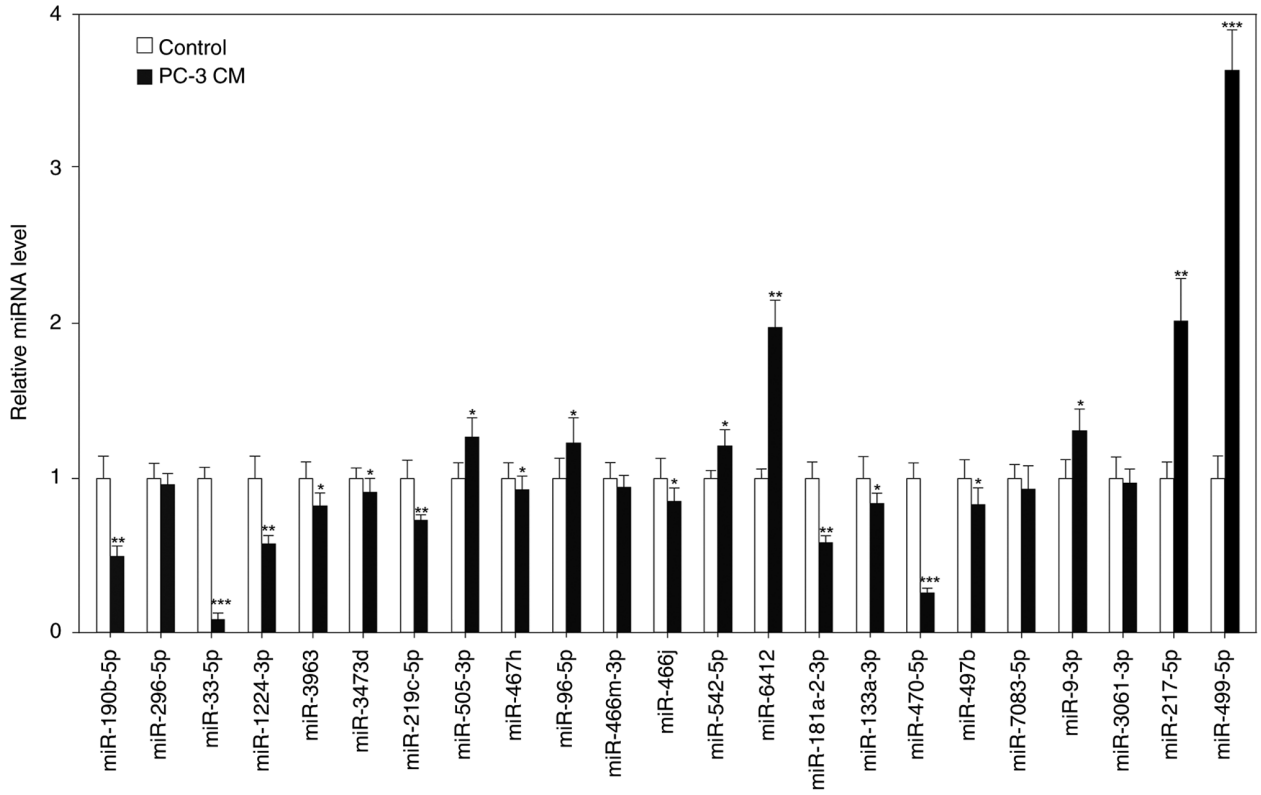

Figure 3. Expression levels of differentially expressed miRNAs were verified using reverse transcription-quantitative PCR. Seven miRNAs were upregulated (miR-499-5p, miR-217-5p, miR-6412, miR-9-3p, miR-505-3p, miR-96-5p, miR-542-5p) and 12 were downregulated (miR-467h, miR-3473d, miR-466j, miR-497b miR-3963, miR-133a-3p, miR-219c-5p, miR-181a-2-3p, miR-1224-3p, miR-190b-5p, miR-470-5p, miR-33-5p), consistent with the results of sequencing. *P<0.05, **P<0.01 and ***P<0.001 vs. control. CM, conditioned medium; miRNA/miR, microRNA.

miRNA-mRNA regulatory network. Among the differentially expressed mRNAs, the potential targets of the differentially expressed miRNAs were predicted by TargetScan database (http://www.targetscan.org), miRDB (http://mirdb.org/) and miRWalk (http://mirwalk.umm.uni-heidelberg.de/). The prediction results of these three types of software were considered the candidate mRNAs of miRNA. The miRNA-mRNA pairs with an inverse expression relationship were included for network construction. The lncRNA-miRNA-mRNA regulatory network was constructed using a combination of lncRNA-miRNA pairs and miRNA-mRNA pairs. Finally, the regulatory network was visualized using Cytoscape 3.4.0 (https://cytoscape.org/).

Bioinformatics analysis. Since miRNAs serve their biological roles through regulating the expression of target genes at the post-transcriptional level, target genes of the miRNAs were predicted using online software, including miRDB (http://www.mirdb.org/), RNA22 (http://cm.jefferson.edu/rna22v2/), TargetScan (http://www.targetscan.org), and miRanda (http://www. microrna.org/). To identify the biological functions of these genes, Kyoto Encyclopedia of Genes and Genomes (KEGG) (https://www.genome.jp/) enrichment analysis were performed. Based on the KEGG database (https://www.genome.jp/), gene sets enriched in the biological pathway associated with osteoblastic differentiation were selected.

Statistical analysis. Experiments were performed in triplicate as a minimum, and data from RT-qPCR, the ALP activity assay and western blotting are presented as the mean ± standard deviation. To identify differentially expressed miRNAs and mRNAs among the groups and to compare differences between groups, unpaired Student's t-test was performed using SPSS 18.0 (IBM Corp.). P<0.05 was considered to indicate a statistically significant difference.

Results

PC-3 CM inhibits osteoblastic differentiation of MC3T3-E1 cells. All of the MC3T3-E1 cells were stimulated with a mechanical tensile strain of 2,500 $\mu\varepsilon$ at 0.5 Hz. Treatment with the PC-3 CM decreased the ALP activity of cells, as well as the mRNA expression levels of collagen, type I, alpha 1 (Col1a1) and osteocalcin (OCN) (Fig. 1A and B). Western blotting indicated that treatment with the PC-3 CM decreased the protein expression levels of RUNX-2 in the MC3T3-E1 cells (Fig. 1C). In addition, the PC-3 CM reduced ALP staining and calcium deposition (Fig. 1D).

PC-3 CM alters the miRNA and mRNA profiles. As shown in Fig. 2, the small RNA sequencing indicated 51 differentially expressed miRNAs (15 upregulated, 36 downregulated). Based on the results of miRNA sequencing, 23 miRNAs were selected from the 51 differentially expressed miRNAs (the top 24 miRNAs demonstrated highly significant differential expression however, one of these had no specific reference sequence). Furthermore, RT-qPCR was used to verify the 23 differentially expressed miRNAs between the physiological

Figure 4. Heat map of differentially expressed mRNAs from MC3T3-E1 cells subjected to mechanical tensile strain and treated with PC-3 CM, as determined by RNA sequencing. Control group, stimulated with mechanical strain; PC-3 CM group, stimulated with mechanical strain and treated with PC-3 CM. The colors represent relative levels of mRNAs. CM, conditioned medium.

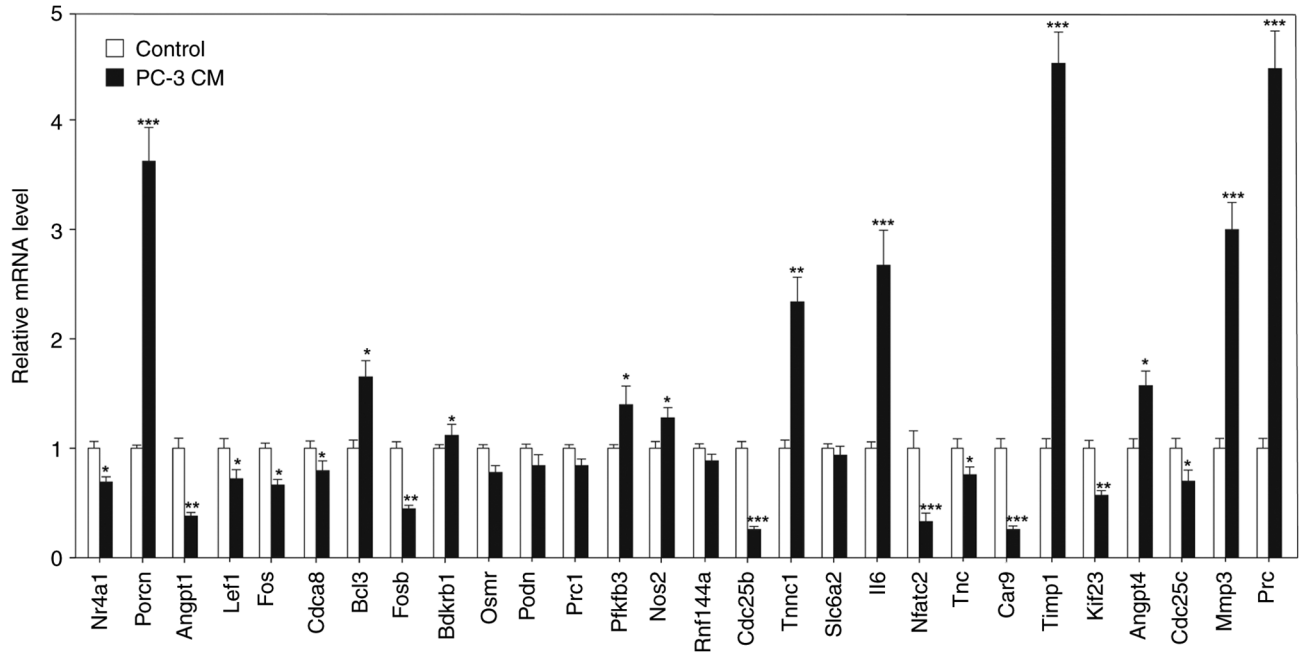

Figure 5. Expression levels of differentially expressed mRNAs were verified using reverse transcription-quantitative PCR. A total of 10 mRNAs were upregulated (Bcl3, Pfkfb3, Mmp3, Bdkrb1, Nos2, Tnnc1, Il6, Timp1, Angpt4, Porcn) and 11 were downregulated (Angpt1, Lef1, Nfatc2, Tnc, Cdc25b, Nr4a1, Fos, Cdca8, Fosb, Kif23, Cdc25c), consistent with the results of sequencing. *P<0.05, **P<0.01 and ***P<0.001 vs. control. CM, conditioned medium.

and pathological groups. The results indicated that seven miRNAs were significantly upregulated and 12 were significantly downregulated, which is consistent with the results of sequencing (Fig. 3).

As shown in Fig. 4, the mRNA sequencing indicated 153 differentially expressed mRNAs (77 upregulated, 76 downregulated). Furthermore, the RNA22 (selection criteria: miR22 score >97.0), TargetScan (selection criteria: Target Scan score >99.0) and miRDB (selection criteria: miRDB score >95.0) databases were used to explore the potential miRNA-mRNA interactions of the differentially expressed miRNAs and mRNAs. Potential miRNA-mRNA interactions of miRNAs were assessed using the three, RNA22, TargetScan and miRDB databases. By combining the results from the three databases and 153 differentially expressed genes from mRNA sequencing, 28 genes were selected for further verification using RT-qPCR. The trend observed in mRNA sequencing for 10 upregulated and 11 downregulated mRNAs was consistent with the RT-qPCR results (Fig. 5).

PC-3 CM alters the lncRNA profile and construction of the ceRNA network. As shown in Fig. 6, RNA sequencing indicated 133 differentially expressed lncRNAs (81 upregulated, 52 downregulated). Furthermore, a ceRNA regulatory network was constructed based on the differentially expressed mRNAs-miRNAs-lncRNAs.

As shown in Fig. 7, 20 differentially expressed miRNAs were selected as core nodes, 6 differentially expressed mRNAs were selected as candidate target genes based on miRDB, TargetScan and miRWalk, and 28 differentially expressed lncRNAs were selected as miRNA sponges according to miRanda, pictar and RNAhybrid. The results suggested that LncRNAs act as ceRNAs to regulate mRNAs by sponging their shared miRNAs.

Prediction of target genes of the differentially expressed miRNAs and signaling pathways involved in osteoblastic differentiation caused by CM. The KEGG enrichment analyses predicted certain signaling pathways were associated with osteoblastic differentiation, including 'Wnt signaling pathway', 'MAPK signaling pathway', 'Calcium signaling pathway', 'Osteoclast differentiation', 'Pathways in cancer', 'TNF signaling pathway', 'HIF-1 signaling pathway', 'MicroRNAs in cancer' and 'Rheumatoid arthritis' (Table III). These signaling pathways may be associated with 'pathological' osteoblastic differentiation (21-28) induced by the CM of PC-3 prostate cancer cells.

Based on the RT-qPCR results of miRNAs and mRNAs, and KEGG analysis, the complete targeting regulatory relationships of mRNAs, miRNAs and signaling pathways were listed. Seven differently expressed mRNAs, and associated miRNAs and signaling pathways were selected (Table IV), which reflect a large range of regulation in the network diagram.

Discussion

Bone is responsive to dynamic mechanical loading; a suitable dynamic mechanical loading maintains the dynamic balance of bone formation (29,30). Osteoblasts, which are located on the surface of bone tissue, are bone-forming cells, which are usually stimulated by dynamic mechanical strain *in vivo* (31). Using a four-point-bend loading device, MC3T3-E1 osteoblastic cells were stimulated with a mechanical tensile strain of 2,500 $\mu\varepsilon$ at 0.5 Hz and were simultaneously treated with PC3 CM, after which the effects of the CM on MC3T3-E1 cells were studied. Treatment with the PC-3 CM inhibited osteoblast differentiation of MC3T3-E1 cells as indicated by the down-regulated expression markers of osteogenic

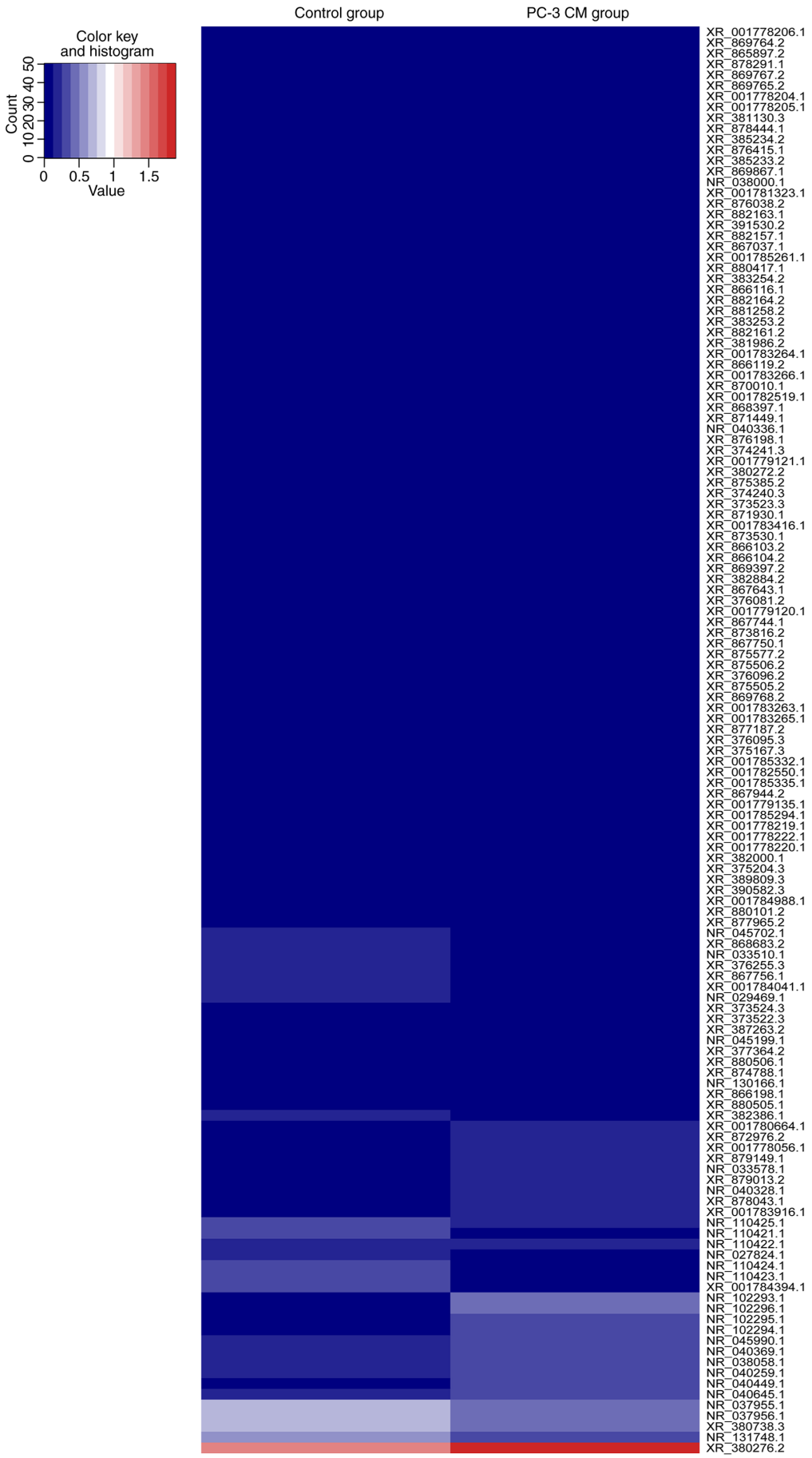

Figure 6. Heat map of differentially expressed lncRNAs from MC3T3-E1 cells subjected to mechanical tensile strain and treated with PC-3 CM, as determined by RNA sequencing. Control group, stimulated with mechanical strain; PC-3 CM group, stimulated with mechanical strain and treated with PC-3 CM. The colors represent relative levels of lncRNAs. CM, conditioned medium; lncRNA, long non-coding RNA.

Table IV. Targeting regulatory relationships among mRNAs, miRNAs and signaling pathways based on the results of reverse transcription-quantitative PCR and Kyoto Encyclopedia of Genes and Genomes analysis.

miRNA		Gene		
Up	Down	Up	Down	Signaling pathway
miR-466j, miR-33-5p			Angpt1	'HIF-1 signaling pathway', 'Rheumatoid arthritis'
miR-96-5p	miR-6412, miR-467h		Cdc25b	'MAPK signaling pathway', 'MicroRNAs in cancer'
miR-505-3p			Lef1	'Wnt signaling pathway', 'pathway in cancer'
miR-33-5p	miR-3473,d miR-1224-3p		Nfactd2	'Wnt signaling pathway', 'Osteoclast differentiation'
miR-219c-5p	miR-1224-3p, miR-542-5p		Tnc	'MicroRNAs in cancer'
miR-466j		Bcl3		'TNF signaling pathway'
miR-3473d, miR-217-5p, miR-133a-3p, miR-1224-3p		Pfkfb3		'HIF-1 signaling pathway'

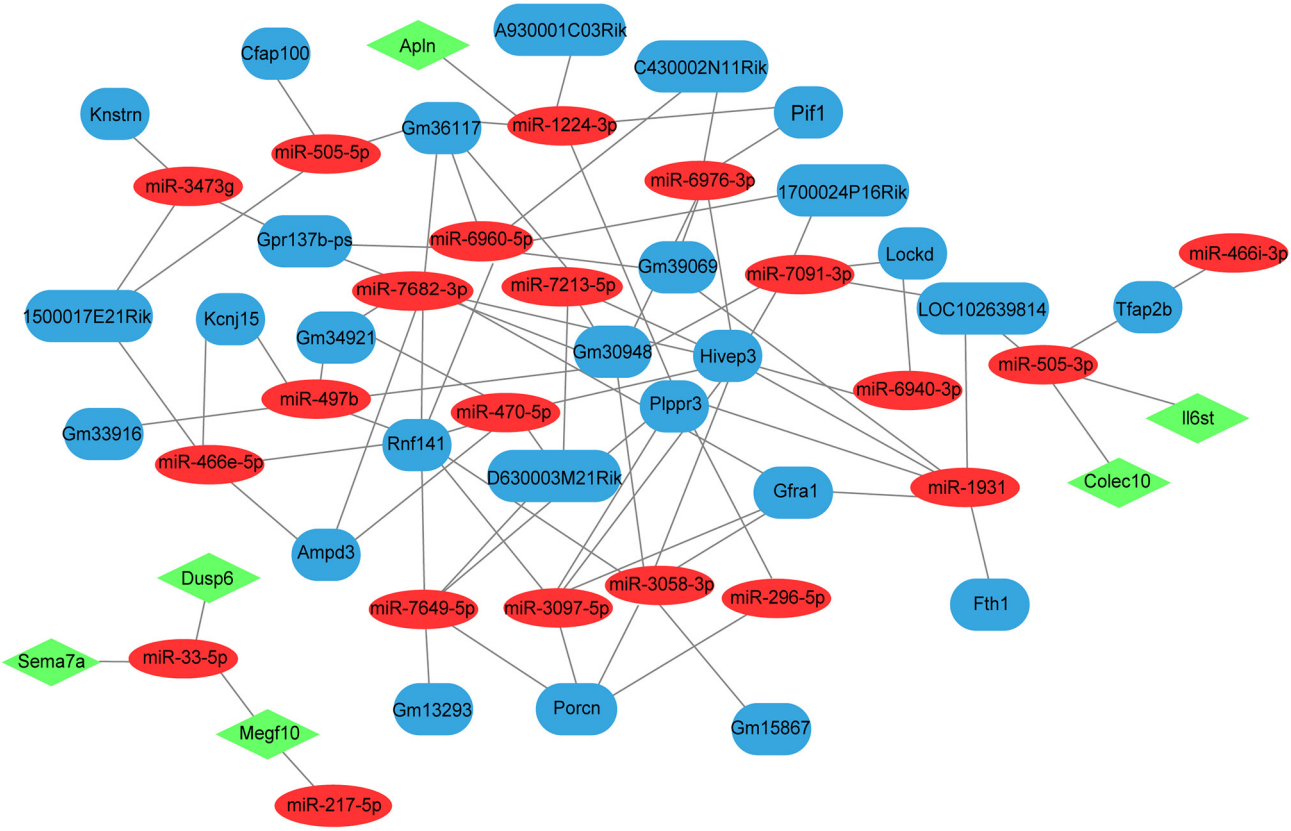

Figure 7. lncRNA-miRNA-mRNA ceRNA network based on sequencing. Red ovals represents miRNAs, green rhombuses represent mRNAs, blue ovals represent lncRNAs. lncRNA, long non-coding RNA; miRNA/miR, microRNA; ceRNA, competing endogenous RNA.

differentiation, and the differentially expressed miRNAs and mRNAs of MC3T3-E1 cells treated with PC-3CM were potentially involved in bone metabolism during prostate cancer progression and bone metastasis.

In the present study, ALP activity, the mRNA expression levels of Col I and OCN, calcium deposition and the protein expression levels of Runx-2 in MC3T3-E1 cells were all decreased in the pathology group, which was treated with the PC-3 CM. These results indicated that the PC-3 CM inhibited the osteogenic differentiation of MC3T3-E1 cells *in vitro*, suggesting that the secretions of PC-3 cells impeded osteogenic differentiation. Subsequently, next generation sequencing was

used to analyze the miRNA and mRNA expression profiles of the pathological and physiological groups. The results showed that, compared with in the physiological group, there were 51 differentially expressed miRNAs and 153 differentially expressed mRNAs in the pathological group.

Furthermore, bioinformatics analysis identified 23 miRNAs and 28 mRNAs from the differential expression profiles and verified them with RT-qPCR. Compared with in the physiological group, there were seven upregulated and 12 downregulated miRNAs, and 10 upregulated and 11 downregulated mRNAs, which were consistent with the results of next generation sequencing. The predicted target mRNAs of the differentially expressed miRNAs implied potential regulatory mechanisms of the miRNA targets in osteoblastic differentiation resulting from the treatment of PC-3 CM.

Moreover, the differentially expressed mRNAs and miRNA-predicted 'target' genes were matched to strengthen the significance of the selected genes and miRNAs, these genes and miRNAs mediated osteoblastic differentiation which was the result of treatment of PC-3 CM. In addition, nine potential pathways, which may be involved in bone metabolism during prostate cancer progression and bone metastasis, were revealed, as follows: 'Wnt signaling pathway', 'MAPK signaling pathway', 'Calcium signaling pathway', 'Osteoclast differentiation', 'Pathways in cancer', 'TNF signaling pathway', 'HIF-1 signaling pathway', 'MicroRNAs in cancer', 'Rheumatoid arthritis'. Relevant literature have demonstrated that these nine pathways are all associated with cancer progression or osteoblastic differentiation (21-28,32,33).

At present, evidence has supported the 'seed and soil' model by Paget, which proposes a specific and strong interaction between metastatic prostate cancer cells and the bone microenvironment (34). Notably, cancer-derived exosomes serve an important role in microenvironment transformation (35). Cancer cells have been reported to secrete a large number of exosomes, which are rich in miRNAs and mRNAs that can enter the target cells and affect their physiological functions (36). The present study generated a model of prostate cancer bone metastasis under mechanical loading, and the differentially expressed miRNAs and mRNAs were detected in osteoblasts. These differentially expressed miRNAs and mRNAs may be mediated by exosomes secreted by prostate cancer.

Currently, widely used cell lines for prostate cancer research include PC3, DU145 or LNCaP cells (37). hFOB 1.19 and MC3T3-E1 cell lines are widely used for osteogenic differentiation studies (38). Since the MC3T3 cell line was used in a previous study of osteogenic differentiation under a physiologically dynamic environment, the present study also used the MC3T3 cell line (17). The present study did not use multiple prostate cancer cell lines, multiple osteoblast cell lines or cell lines of human origin, which was a limitation. The present study does not fully reflect the bone metastasis of prostate cancer, but it does provide ideas for the study of the mechanism of bone metastasis in prostate cancer.

The present findings suggested that genetic interactions (miRNA-gene-signaling pathway) may be associated with the bone metastasis of prostate cancer. Molecular alterations in gene expression may therefore represent a novel signature in pathological osteoblastic differentiation of prostate cancer, which could be used to develop diagnostic and therapeutic strategies for patients with prostate cancer and pathological osteoblastic differentiation caused by bone metastasis. However, these target genes and miRNAs require further verification in subsequent studies, and the mechanism underlying the involvement of differentially expressed miRNAs and genes in the osteoblasts after bone metastasis of prostate cancer also need further investigation.

Acknowledgements

Not applicable.

Funding

The work was supported by the National Nature Science Foundation of China (grant nos. 31660261 and 12202113) and the Natural Science Foundation of Guangxi (grant nos. 2018GXNSFAA281357 and 2016GXNSFAA380322).

Availability of data and materials

The datasets used and/or analyzed during the current study are available from the corresponding author on reasonable request. The sequencing datasets generated and/or analyzed during the current study are available in the Gene Expression Omnibus repository (https://www.ncbi.nlm.nih.gov/geo/query/acc.cgi?acc=GSE211413).

Authors' contributions

YG designed the study, analyzed the data and participated in the bioinformatics analysis. ZC performed all the RT-qPCR analyses at Guangzhou RiboBio Co., Ltd. (experimental equipment and most of the reagents were provided by Guangzhou RiboBio Co., Ltd.). ZXY performed ALP activity and Alizarin red-S staining. JHW performed western blotting. HY, BH and JTG performed the bioinformatics analysis. YG and ZC wrote and revised the manuscript. YG and ZC confirm the authenticity of all the raw data. All authors have read and approved the final manuscript.

Ethics approval and consent to participate

Not applicable.

Patient consent for publication

Not applicable.

Competing interests

The authors declare that they have no competing interests.

References

1. Molla MS, Katti DR, Iswara J, Venkatesan R, Paulmurugan R and Katti KS: Prostate cancer phenotype influences bone mineralization at metastasis: A study using an in vitro prostate cancer metastasis testbed. JBMR Plus 4: e10256, 2020.

2. Liu X, Chen L, Fan Y, Hong Y, Yang X, Li Y, Lu J, Lv J, Pan X, Qu F, *et al*: IFITM3 promotes bone metastasis of prostate cancer cells by mediating activation of the TGF-β signaling pathway. Cell Death Dis 10: 517, 2019.
3. Quiroz-Munoz M, Izadmehr S, Arumugam D, Wong B, Kirschenbaum A and Levine AC: Mechanisms of osteoblastic bone metastasis in prostate cancer: Role of prostatic acid phosphatase. J Endocr Soc 3: 655-664, 2019.
4. Das SK, Maji S, Wechman SL, Bhoopathi P, Pradhan AK, Talukdar S, Sarkar D, Landry J, Guo C, Wang XY, *et al*: MDA-9/syntenin (SDCBP): Novel gene and therapeutic target for cancer metastasis. Pharmacol Res 155: 104695, 2020.
5. Singla N, Ghandour RA and Raj GV: Investigational luteinizing hormone releasing hormone (LHRH) agonists and other hormonal agents in early stage clinical trials for prostate cancer. Expert Opin Investig Drugs 28: 249-259, 2019.
6. Probert C, Dottorini T, Speakman A, Hunt S, Nafee T, Fazeli A, Wood S, Brown JE and James V: Communication of prostate cancer cells with bone cells via extracellular vesicle RNA; a potential mechanism of metastasis. Oncogene 38: 1751-1763, 2019.
7. Ajdžanovic V, Filipovic B, Miljic D, Mijatovic S, Maksimovic-Ivanic D, Miler M, Živanovic J and Miloševic V: Prostate cancer metastasis and soy isoflavones: A dogfight over a bone. EXCLI J 18: 106-126, 2019.
8. Marques ACP: A diachronic approach to neoplasms: Skeletal evidence fromthe portuguese identified osteological collections (19 th-20 th Centuries): Universidade de Coimbra (Portugal); 2018.
9. Stankiewicz E: Identification of the genetic alterations in prostate cancer metastases: Queen Mary University of London; 2017.
10. Ye Y, Li SL, Ma YY, Diao YJ, Yang L, Su MQ, Li Z, Ji Y, Wang J, Lei L, *et al*: Exosomal miR-141-3p regulates osteoblast activity to promote the osteoblastic metastasis of prostate cancer. Oncotarget 8: 94834-94849, 2017.
11. Wittkowske C, Reilly GC, Lacroix D and Perrault CM: In vitro bone cell models: Impact of fluid shear stress on bone formation. Front Bioeng Biotechnol 4: 87, 2016.
12. Hart NH, Nimphius S, Rantalainen T, Ireland A, Siafarikas A and Newton R: Mechanical basis of bone strength: Influence of bone material, bone structure and muscle action. J Musculoskelet Neuronal Interact 17: 114-139, 2017.
13. Frost HM: Perspectives: A proposed general model of the 'mechanostat' (suggestions from a new skeletal-biologic paradigm). Anat Rec 244: 139-147, 1996.
14. Mueller SM, Herter-Aeberli I, Cepeda-Lopez AC, Flück M, Jung HH and Toigo M: The effect of body composition and serum inflammatory markers on the functional muscle-bone unit in premenopausal women. Int J Obes (Lond) 41: 1203-1206, 2017.
15. Liu Q, Guo Y, Wang Y, Zou X and Yan Z: MiR-98-5p promotes osteoblast differentiation in MC3T3-E1 cells by targeting CKIP-1. Mol Med Rep 17: 4797-4802, 2018.
16. Guo Y, Zhang CQ, Zeng QC, Li RX, Liu L, Hao QX, Shi CH, Zhang XZ and Yan YX: Mechanical strain promotes osteoblast ECM formation and improves its osteoinductive potential. Biomed Eng Online 11: 80, 2012.
17. Guo Y, Wang Y, Liu Y, Liu Y, Zeng Q, Zhao Y, Zhang X and Zhang X: MicroRNA-218, microRNA-191*, microRNA-3070a and microRNA-33 are responsive to mechanical strain exerted on osteoblastic cells. Mol Med Rep 12: 3033-3038, 2015.
18. Mackowiak SD: Identification of novel and known miRNAs in deep-sequencing data with miRDeep2. Curr Protoc Bioinformatics 36: 12.10. 1-12.10. 15, 2011.
19. Wang L and Wang X: DEGseq: Identify differentially expressed genes from RNA-seq data J R package version 1. 24, 2016.
20. Livak KJ and Schmittgen TD: Analysis of relative gene expression data using real-time quantitative PCR and the 2(-Delta Delta C(T)) method. Methods 25: 402-408. 2001.
21. Han C, Li J, Wang C, Ouyang H, Ding X, Liu Y, Chen S and Luo L: Wnt5a Contributes to the differentiation of human embryonic stem cells into lentoid bodies through the noncanonical Wnt/JNK signaling pathway. Invest Ophthalmol Vis Sci 59: 3449-3460, 2018.
22. Ma S, Liu G, Jin L, Pang X, Wang Y, Wang Z, Yu Y and Yu J: IGF-1/IGF-1R/hsa-let-7c axis regulates the committed differentiation of stem cells from apical papilla. Sci Rep 6: 36922, 2016.
23. Chen D, Wu L, Liu L, Gong Q, Zheng J, Peng C and Deng J: Comparison of HIF1A-AS1 and HIF1A-AS2 in regulating HIF-1α and the osteogenic differentiation of PDLCs under hypoxia. Int J Mol Med 40: 1529-1536, 2017.
24. Han P, Lloyd T, Chen Z and Xiao Y: Proinflammatory cytokines regulate cementogenic differentiation of periodontal ligament cells by Wnt/Ca2+ signaling pathway. J Interferon Cytokine Res 36: 328-337, 2016.
25. Cheng J, Yang K, Zhang Q, Yu Y, Meng Q, Mo N, Zhou Y, Yi X, Ma C, Lei A and Liu Y: The role of mesenchymal stem cells in promoting the transformation of androgen-dependent human prostate cancer cells into androgen-independent manner. Sci Rep 6: 16993, 2016.
26. Wang YJ, Zhang HQ, Han HL, Zou YY, Gao QL and Yang GT: Taxifolin enhances osteogenic differentiation of human bone marrow mesenchymal stem cells partially via NF-κB pathway. Biochem Biophys Res Commun 490: 36-43, 2017.
27. Yu Y, Ma L, Zhang H, Sun W, Zheng L, Liu C and Miao L: EPO could be regulated by HIF-1 and promote osteogenesis and accelerate bone repair. Artif Cells Nanomed Biotechnol 48: 206-217, 2020.
28. Huang X, Xiong X, Liu J, Zhao Z and Cen X: MicroRNAs-containing extracellular vesicles in bone remodeling: An emerging frontier. Life Sci 254: 117809, 2020.
29. Yan Y, Sun H, Gong Y, Yan Z, Zhang X, Guo Y and Wang Y: Mechanical strain promotes osteoblastic differentiation through integrin-β1-mediated β-catenin signaling. Int J Mol Med 38: 594-600, 2016.
30. Betti BF, Everts V, Ket JC, Tabeian H, Bakker AD, Langenbach GE and Lobbezoo F: Effect of mechanical loading on the metabolic activity of cells in the temporomandibular joint: A systematic review. Clin Oral Investig 22: 57-67, 2018.
31. Piet J, Hu D, Baron R and Shefelbine SJ: Bone adaptation compensates resorption when sciatic neurectomy is followed by low magnitude induced loading. Bone 120: 487-494, 2019.
32. Robertson-Anderson R: Nonlinear microscale mechanics and macromolecular mobility of tunable cytoskeleton composites. Aps March Meeting; 2019.
33. Kasoha M, Bohle RM, Seibold A, Gerlinger C, Juhasz-Böss I and Solomayer EF: Dickkopf-1 (Dkk1) protein expression in breast cancer with special reference to bone metastases. Clin Exp Metastasis 35: 763-775, 2018.
34. Paget S: The distribution of secondary growths in cancer of the breast. 1889. Cancer Metastasis Rev 8: 98-101, 1989.
35. Wang H, Yung MMH, Ngan HYS, Chan KKL and Chan DW: The impact of the tumor microenvironment on macrophage polarization in cancer metastatic progression. Int J Mol Sci 22: 6560, 2021.
36. Jiang X, You L, Zhang Z, Cui X, Zhong H, Sun X, Ji C and Chi X: Biological properties of milk-derived extracellular vesicles and their physiological functions in infant. Front Cell Dev Biol 9: 693534, 2021.
37. Su CY, Huang GC, Chang YC, Chen YJ and Fang HW: Analyzing the expression of biomarkers in prostate cancer cell lines. In vivo 35: 1545-1548, 2021.
38. Kazimierczak P, Vivcharenko V, Truszkiewicz W, Wójcik M and Przekora A: Osteoblasts response to novel chitosan/agarose/hydroxyapatite bone scaffold-studies on MC3T3-E1 and HFOB 1.19 cellular models. Engineering Biomaterials 151: 24-29, 2019.